

# UCTransNet: Rethinking the Skip Connections in U-Net from a Channel-wise Perspective with Transformer

Haonan Wang<sup>1</sup>, Peng Cao<sup>1\*</sup>, Jiaqi Wang<sup>1</sup>, Osmar R. Zaiane<sup>2</sup>

<sup>1</sup> College of Computer Science and Engineering, Key Laboratory of Intelligent Computing in Medical Image, Northeastern University, Shenyang, China

<sup>2</sup> Amii, University of Alberta, Edmonton, Canada

haonan1wang@gmail.com, caopeng@mail.neu.edu.com, wjq010222@gmail.com, zaiane@cs.ualberta.ca

## Abstract

Most recent semantic segmentation methods adopt a U-Net framework with an encoder-decoder architecture. It is still challenging for U-Net with a simple skip connection scheme to model the global multi-scale context: 1) Not each skip connection setting is effective due to the issue of incompatible feature sets of encoder and decoder stage, even some skip connection negatively influence the segmentation performance; 2) The original U-Net is worse than the one without any skip connection on some datasets. Based on our findings, we propose a new segmentation framework, named UC-TransNet (with a proposed CTrans module in U-Net), from the channel perspective with attention mechanism. Specifically, the CTrans (Channel Transformer) module is an alternate of the U-Net skip connections, which consists of a sub-module to conduct the multi-scale Channel Cross fusion with Transformer (named CCT) and a sub-module Channel-wise Cross-Attention (named CCA) to guide the fused multi-scale channel-wise information to effectively connect to the decoder features for eliminating the ambiguity. Hence, the proposed connection consisting of the CCT and CCA is able to replace the original skip connection to solve the semantic gaps for an accurate automatic medical image segmentation. The experimental results suggest that our UCTransNet produces more precise segmentation performance and achieves consistent improvements over the state-of-the-art for semantic segmentation across different datasets and conventional architectures involving transformer or U-shaped framework. Code: <https://github.com/McGregorWwww/UCTransNet>.

## Introduction

Medical imaging is considered as a vital technique to assist doctors to evaluate disease and to optimise prevention and control measures. Segmentation and the subsequent quantitative assessment of target object in medical images provide valuable information for the analysis of pathologies and are important for planning of treatment strategies, monitoring of disease progression and prediction of patient outcome. Recent approaches (Long, Shelhamer, and Darrell 2015; Ni et al. 2020; Wen, Xie, and He 2020) to semantic segmentation typically rely on convolutional encoder-decoder architectures where the encoder generates low-resolution image features and the decoder upsamples features to segmentation maps with per pixel class scores. U-Net (Ronneberger,

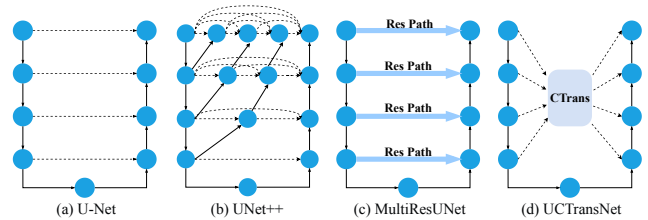


Figure 1: Comparison of the skip connection scheme among the proposed UCTransNet (d) and other models.

Fischer, and Brox 2015) is the most widely used encoder-decoder network architecture for medical image segmentation, since the encoder captures the low-level and high-level features, and the decoder combines the semantic features to construct the final result. The skip connection can help propagate the spatial information that gets lost during the pooling operation to help recover the full spatial resolution through the encoding-decoding process. To investigate it, we conduct an in-depth study of U-Net and observe several major limitations according to our analysis on multiple datasets. We find that it is still challenging for U-Net with a simple skip connection scheme to model the global multi-scale context for assisting the decoding process without considering the semantic gap. It is necessary to find an effective way to fuse features for precise medical image segmentation. There essentially are two key issues for the extension of U-Net: which layers of the features in the encoders are connected to the decoders for modeling a global contexts through aggregating multi-scale features, and how to effectively fuse the features with possible semantic gap instead of simply concatenating? There exist two semantic gaps: semantic gap among the multi-scale encoder features and between the stages of the encoder and decoder, limiting the segmentation performance. To overcome this aforementioned limitation, a number of approaches have been introduced recently to alleviate the discrepancy when fusing these two incompatible sets of features. One approach is to directly replace the plain skip connections with the nested dense skip pathways for medical image segmentation. The most representative method is UNet++ (Zhou et al. 2018) which narrows the semantic gap between the encoder and decoder sub-networks by introducing dense connectivity with a series of convolu-

\*Corresponding author.

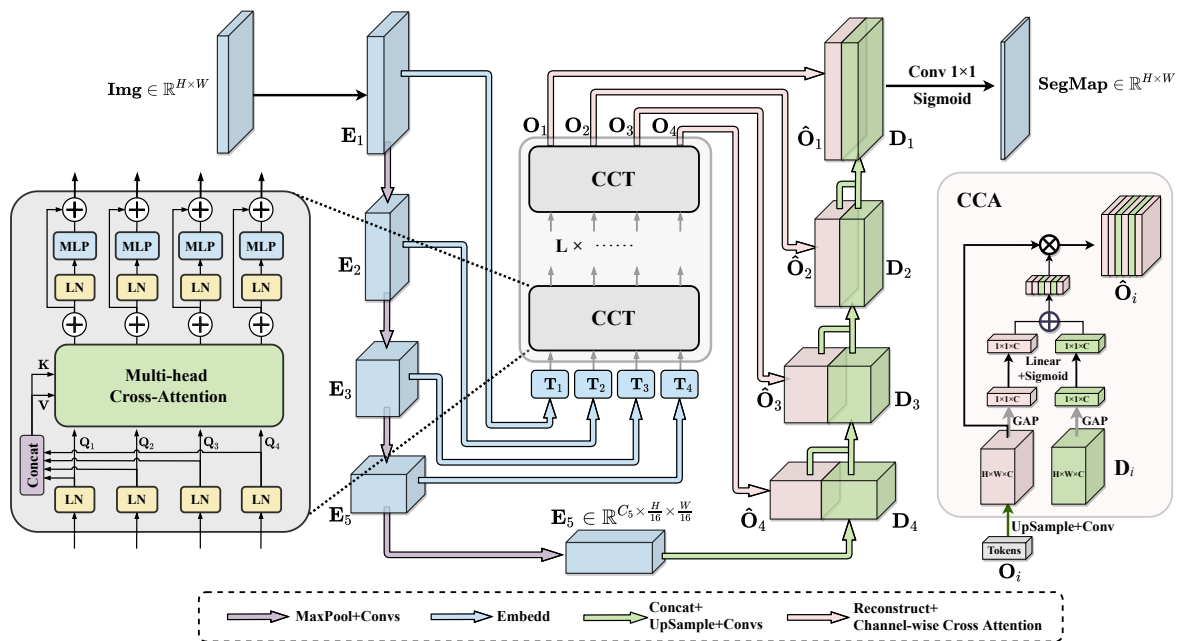


Figure 2: Illustration of the proposed UTransNet. We replace the original skip connections by CTrans consisting of two components: Channel-wise Cross fusion Transformer (CCT) and Channel-wise Cross Attention (CCA).

tions and achieves better segmentation performance. It is an improvement over the restrictive skip connections in U-Net requiring the fusion of only same-scale feature maps. The other approach focuses on strengthening the skip connections by introducing additional non-linear transformations on the features propagating from the encoder stage, which should account for or somewhat balance the possible semantic gaps (Rahman 2020).

Despite achieving good performance, both works above are still incapable of effectively exploring sufficient information from full scales. Capturing multi-scale features is essential for resolving complex scale variations in medical image segmentation. Driven by the important issues, a question arises: how to sufficiently bridge the semantic gap between the encoder and decoder through multi-scale channel-wise information fusion by effectively capturing the non-local semantic dependencies. In this paper, we rethink the skip connection design and propose an alternative method for better connecting the features between the encoder and decoder stages. Different channels usually focus on different semantic patterns, adaptively fusing sufficient channel-wise features is favorable for the complex medical image segmentation. To this end, we propose an end-to-end deep learning network called UTransNet, which takes U-Net as the main structure of the network. More specifically, we firstly propose a Channel-wise Cross Fusion Transformer (CCT) to fuse the multi-scale context with cross attention from the channel-wise perspective. It aims at capturing local cross-channel interaction to achieve an adaptive scheme for effectively fusing the multi-scale channel-wise features with possible scale semantic gap through collaborative learning rather than independent connection. On the other hand, we

propose another channel-wise cross attention (CCA) module for fusing the fused multi-scale features and the features from decoder stages to solve the inconsistent semantic level. Both cross attention modules are called CTrans (Channel Transformer), which can establish the association between encoder and decoder by exploring the multi-scale global context and replace the original skip connections to solve the semantic gaps for improved segmentation performances. Both proposed modules can be easily embedded in and applied for the U-shape networks in medical image segmentation tasks. Extensive experiments show that UTransNet can greatly improve conventional segmentation pipelines by the following absolute gains of 4.05% Dice, 7.98% Dice and 9.00% Dice over U-Net on GlAS, MoNuSeg and Synapse datasets, respectively. Moreover, we made a thorough analysis to investigate how the feature interactions work. Besides, previous works have combined both Transformers and U-Net to explicitly model long-range spatial dependency (Chen et al. 2021; Zhang, Liu, and Hu 2021). The results demonstrate that channel-wise fusion transformer scheme generally leads to a better performance than the methods incorporating the transformer to replace the convolution operation. We argue that UTransNet can serve as strong skip connection scheme for medical image segmentation.

Our contributions are three-fold. 1) We analyze the effectiveness of skip connections on multiple datasets, indicating that the independent simple copying is not appropriate. 2) We suggest a new perspective to boost semantic segmentation performance, i.e. bridging the semantic and resolution gap between low-level and high-level features by a more effective feature fusion with multi-scale channel-wise cross attention for capturing more sophisticated channel-wise de-

dependencies. 3) To the best of our knowledge, the proposed UCTransNet is the first method to rethink the self-attention mechanism of Transformer in a channel-wise perspective. In comparison to other state-of-the-art segmentation methods, our experimental results present better performances on all the three public datasets.

## Related Works

### Transformers for Medical Image Segmentation

Recently, Vision Transformer (ViT) (Dosovitskiy et al. 2020) achieved state-of-the-art on ImageNet classification by directly applying Transformers with global self-attention to full-sized images. Due to the success of Transformers in many computer vision fields, a new paradigm for medical image segmentation has recently evolved (Zheng et al. 2020; Zhang et al. 2021; Gao et al. 2021; Ji et al. 2021; Gao, Zhou, and Metaxas 2021; Zhang, Liu, and Hu 2021; Hatamizadeh et al. 2021). TransUNet (Chen et al. 2021) is the first Transformer-based medical image segmentation framework. Valanarasu et al. proposed a Gated Axial-Attention model—MedT (Valanarasu et al. 2021) to overcome the low number of data samples in medical imaging. Motivated by Swin Transformer (Liu et al. 2021) which achieved state-of-the-art performance, Swin-Unet (Cao et al. 2021) proposed the first pure Transformer-based U-shaped architecture which introduced Swin Transformer to replace the convolution blocks in U-Net. However, the aforementioned methods mainly focus on the defects of convolution operation rather than the U-Net it-self, thus may cause structural redundancy and prohibitive computational cost.

### Skip Connections in U-shaped Nets

The skip connection mechanism was first proposed in U-Net (Ronneberger, Fischer, and Brox 2015), which was designed to bridge the semantic gap between encoder and decoder, and have proven to be effective in recovering fine-grained details of the target objects (Drozdal et al. 2016; He et al. 2016; Huang et al. 2017). Following the popularity of U-Net, many novel models have been proposed such as UNet++ (Zhou et al. 2018), Attention U-Net (Oktay et al. 2018), DenseUNet (Li et al. 2018), R2U-Net (Alom et al. 2018), and UNet 3+ (Huang et al. 2020), which are specially designed for medical image segmentation and achieve expressive performance. Zhou et al. (Zhou et al. 2018) believed that the same-scale feature maps from the encoder and decoder networks are semantically dissimilar and thus designed a nested structure named UNet++ which captures multi-scale features to further bridge the gap. Attention-UNet proposed cross-attention module which uses coarse-scale features as gating signals to disambiguate irrelevant and noisy responses in skip connections. MultiResUNet (Rahman 2020) observed a possible semantic gap between the skipped encoder features and the decoder features in the same level, thus they introduced the Res Path with residual structure to improve the skip connections (see Fig. 1).

These methods assume that each skip connection has equal contribution, however in the next section we will show

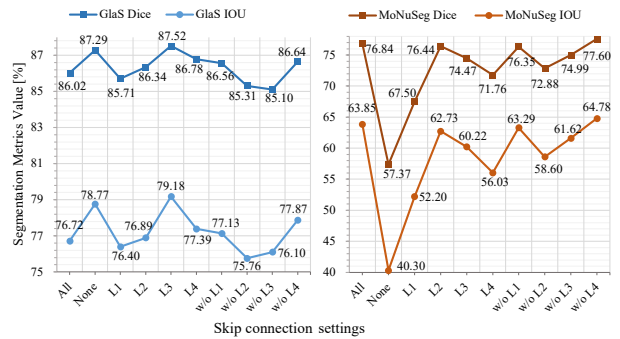


Figure 3: Analysis of different skip connection layers of U-Net. ‘All’ represents the original U-Net, ‘L1’ represents only the skip connection of level one is kept and ‘w/o L1’ represents only the skip connection of level one is removed.

that the contributions are different among all the skip connections, some may even harm the final performance.

### The Analysis of Skip connection

In this section, we thoroughly analyze the contribution of the Skip connection to the segmentation performance on the datasets of Glas and MoNuSeg. According to the analysis, three findings are highlighted as follows:

**Finding 1:** The U-net without any skip connection is even better than the original U-Net. Comparing the results of Fig. 3, we can find that ‘U-Net-none’ shows the worst performance among the algorithms for almost all metrics on the MoNuSeg dataset. However, ‘U-Net-none’, although without any constraints, still achieves very competitive performance against ‘U-Net-all’ on the Glas dataset. It demonstrates that the skip connection is not always beneficial for the segmentation.

**Finding 2:** Although UNet-all performs better than UNet-none, not all skip connections with simple copying are useful for segmentation. The contribution of each skip connection is different. We find that the performance range of each skip connection is [67.5%,76.44%] and [52.2%,62.73%] with respect to Dice and IOU on the MoNuSeg dataset. The impact variation is large for the different single skip connection. Furthermore, due to the issue of incompatible feature sets of the encoder and decoder stages, some skip connection negatively influence the segmentation performance. For example,  $L_1$  performs worse than UNet-none in terms of Dice and IOU on the Glas dataset. The result does not demonstrate that many features from the encoder stage are not informative. The reason behind it may be that the simple copying is not appropriate for the feature fusion.

**Finding 3:** The optimal combination of skip contributions is different for different datasets, which depends on the scales and appearance of the target lesions. We run several ablation experiments to explore the best side output settings. Note that we ignore the combination of two skip connections due to the limited space. As can be seen, the skip connections does not achieve better performance. The

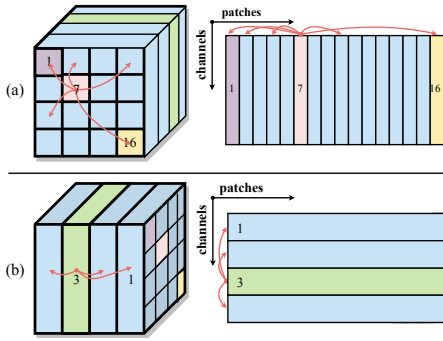


Figure 4: Comparison between the original self-attention (a) and our proposed channel-wise cross-attention (b).

model w/o  $L_4$  is best on the MoNuSeg dataset, whilst to our surprise, the  $L_3$  with only one skip connection performs best on the GlaS dataset. These observations suggest that the optimal combination is different for different datasets. This further confirms the necessity of introducing more appropriate course of action for the feature fusion rather than simple connection.

## UCTransNet for Medical Image Segmentation

Fig. 2 illustrates an overview of our UCTransNet framework. To the best of our knowledge, current Transformer-based segmentation methods mainly focus on improving the encoder of U-Net, based on its advantage of capturing long-range information. These methods, such as TransUNet (Chen et al. 2021) or TransFuse (Zhang, Liu, and Hu 2021), blend the Transformer with U-Net in a simple way, i.e. plugging the Transformer module into the encoder or fusing the both independent branches. However, we believe the potential limitation of the current U-Net model is the issue of the skip connection rather than the encoder of the original U-Net, which is sufficient for the most tasks. As mentioned in the section of skip connection analysis, we observe that the feature from the encoder is inconsistent with that from the decoder, i.e. in some cases, the shallower layer features with less semantic information may harm the final performance through the simple skip connection due to the semantic gap between the shallower level encoder and decoder. Inspired by it, we construct the UCTransNet framework by designing a channel-wise Transformer module between the vanilla U-Net encoder and decoder to better fuse the encoder features and reduce the semantic gap. Specifically, we propose a Channel Transformer (CTrans) to replace the skip connections in U-Net, which consists of two modules: CCT (Channel-wise Cross Fusion Transformer) for the multi-scale encoder feature fusion and CCA (Channel-wise Cross Attention) for the fusion of the decoder features and the enhanced CCT features.

### CCT: Channel-wise Cross Fusion Transformer for Encoder Feature Transformation

To solve the skip connection issue mentioned before, we propose a new Channel-wise Cross Fusion Transformer

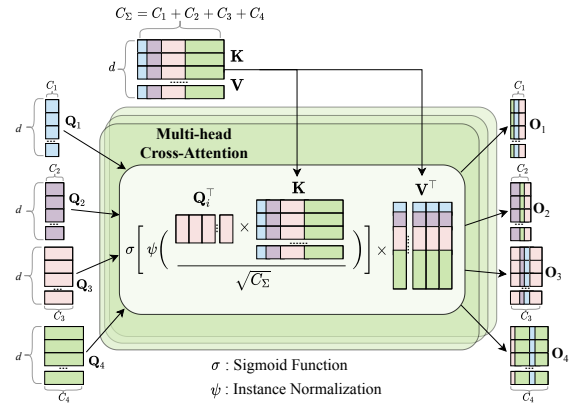


Figure 5: Multi-head Cross-Attention.

(CCT) to fuse the multi-scale encoder features with the advantage of the long dependency modeling in Transformer. The CCT module consists of three steps: multi-scale feature embedding, multi-head channel-wise cross attention and Multi-Layer Perceptron (MLP).

**Multi-scale Feature Embedding** Given the outputs of four skip connection layers  $\mathbf{E}_i \in \mathbb{R}^{\frac{H \times W}{i^2} \times C_i}$ , ( $i = 1, 2, 3, 4$ ), we first perform tokenization by reshaping the features into sequences of flattened 2D patches with patch sizes  $P, \frac{P}{2}, \frac{P}{4}, \frac{P}{8}$  respectively, so that the patches can be mapped to the same areas of the encoder features in four scales. We keep the original channel dimensions through this process. Then, we concatenate the tokens of four layers  $\mathbf{T}_i$  ( $i = 1, 2, 3, 4$ ),  $\mathbf{T}_i \in \mathbb{R}^{\frac{H \times W}{i^2} \times C_i}$  as the key and value  $\mathbf{T}_\Sigma = \text{Concat}(\mathbf{T}_1, \mathbf{T}_2, \mathbf{T}_3, \mathbf{T}_4)$ .

**Multi-head Cross-Attention** The tokens are then fed into the multi-head channel cross-attention module, followed by a Multi-Layer Perceptron (MLP) with residual structure, to encode channel relationships and dependencies for refining features from each U-Net encoder level using multi-scale features.

As shown in Fig. 5, the proposed CCT module contains five inputs, including four tokens  $\mathbf{T}_i$  as queries and a concatenated token  $\mathbf{T}_\Sigma$  as key and value:

$$\mathbf{Q}_i = \mathbf{T}_i \mathbf{W}_{\mathbf{Q}_i}, \mathbf{K} = \mathbf{T}_\Sigma \mathbf{W}_{\mathbf{K}}, \mathbf{V} = \mathbf{T}_\Sigma \mathbf{W}_{\mathbf{V}} \quad (1)$$

where  $\mathbf{W}_{\mathbf{Q}_i} \in \mathbb{R}^{C_i \times d}$ ,  $\mathbf{W}_{\mathbf{K}} \in \mathbb{R}^{C_\Sigma \times d}$ ,  $\mathbf{W}_{\mathbf{V}} \in \mathbb{R}^{C_\Sigma \times d}$  are weights of different inputs,  $d$  is the sequence length (patch numbers) and  $C_i$  ( $i = 1, 2, 3, 4$ ) are the channel dimensions of the four skip connection layers. In our implementation  $C_1 = 64, C_2 = 128, C_3 = 256, C_4 = 512$ .

With  $\mathbf{Q}_i \in \mathbb{R}^{C_i \times d}$ ,  $\mathbf{K} \in \mathbb{R}^{C_\Sigma \times d}$ ,  $\mathbf{V} \in \mathbb{R}^{C_\Sigma \times d}$ , the similarity matrix  $\mathbf{M}_i$  are produced and the value  $\mathbf{V}$  is weighted by  $\mathbf{M}_i$  through a cross-attention (CA) mechanism:

$$\begin{aligned} \text{CA}_i &= \mathbf{M}_i \mathbf{V}^\top = \sigma \left[ \psi \left( \frac{\mathbf{Q}_i^\top \mathbf{K}}{\sqrt{C_\Sigma}} \right) \right] \mathbf{V}^\top \\ &= \sigma \left[ \psi \left( \frac{\mathbf{W}_{\mathbf{Q}_i}^\top \mathbf{T}_i^\top \mathbf{T}_\Sigma \mathbf{W}_{\mathbf{K}}}{\sqrt{C_\Sigma}} \right) \right] \mathbf{W}_{\mathbf{V}}^\top \mathbf{T}_\Sigma^\top \end{aligned} \quad (2)$$

where  $\psi(\cdot)$  and  $\sigma(\cdot)$  denote the instance normalization (Ulyanov, Vedaldi, and Lempitsky 2017) and the soft-max function, respectively.

The major difference from the original self-attention is that we conduct the attention operation along the channel-axis rather than the patch-axis (see Fig. 4), and we employ the instance normalization on the similarity maps so that the gradient can be smoothly propagated. In a  $N$ -head attention situation, the output after multi-head cross-attention is calculated as follow:

$$\text{MCA}_i = (\text{CA}_i^1 + \text{CA}_i^2 + \dots + \text{CA}_i^N) / N \quad (3)$$

where  $N$  is the number of heads. Hereinafter, applying a simple MLP and residual operator, the output is obtained as follows:

$$\mathbf{O}_i = \text{MCA}_i + \text{MLP}(\mathbf{Q}_i + \text{MCA}_i) \quad (4)$$

We omitted the layer normalization (LN) in the equation for simplicity. The operation in Eq. (4) is repeated  $L$  times to build a  $L$ -layer Transformer. In our implementation,  $N$  and  $L$  are both set to 4. Finally, the four outputs of the  $L$ -th layer  $\mathbf{O}_1, \mathbf{O}_2, \mathbf{O}_3$  and  $\mathbf{O}_4$  are reconstructed through an up-sampling operation followed by a convolution layer and concatenated with the decoder features  $\mathbf{D}_1, \mathbf{D}_2, \mathbf{D}_3$  and  $\mathbf{D}_4$ , respectively.

### CCA: Channel-wise Cross Attention for Feature Fusion in Decoder

In order to better fuse features of inconsistent semantics between the Channel Transformer and U-Net decoder, we propose a channel-wise cross attention module, which can guide the channel and information filtration of the Transformer features and eliminate the ambiguity with the decoder features.

Mathematically, we take the  $i$ -th level Transformer output  $\mathbf{O}_i \in \mathbb{R}^{C \times H \times W}$  and  $i$ -th level decoder feature map  $\mathbf{D}_i \in \mathbb{R}^{C \times H \times W}$  as the inputs of Channel-wise Cross Attention. spatial squeeze is performed by a global average pooling (GAP) layer, producing vector  $\mathcal{G}(\mathbf{X}) \in \mathbb{R}^{C \times 1 \times 1}$  with its  $k^{th}$  channel  $\mathcal{G}(\mathbf{X}) = \frac{1}{H \times W} \sum_{i=1}^H \sum_{j=1}^W \mathbf{X}^k(i, j)$ . We use this operation to embed the global spatial information and then generate the attention mask:

$$\mathbf{M}_i = \mathbf{L}_1 \cdot \mathcal{G}(\mathbf{O}_i) + \mathbf{L}_2 \cdot \mathcal{G}(\mathbf{D}_i) \quad (5)$$

where  $\mathbf{L}_1 \in \mathbb{R}^{C \times C}$  and  $\mathbf{L}_2 \in \mathbb{R}^{C \times C}$  and being weights of two Linear layers and the ReLU operator  $\delta(\cdot)$ . This operation in Eq. (5) encodes the channel-wise dependencies. Followed ECA-Net (Wang et al. 2020) which empirically showed avoiding dimensionality reduction is important for learning channel attention, we use a single Linear layer and sigmoid function to build the channel attention map. The resultant vector is used to recalibrate or excite  $\mathbf{O}_i$  to  $\hat{\mathbf{O}}_i = \sigma(\mathbf{M}_i) \cdot \mathbf{O}_i$ , where the activation  $\sigma(\mathbf{M}_i)$  indicates the importance of each channel. Finally, the masked  $\hat{\mathbf{O}}_i$  is concatenated with the up-sampled features of the  $i$ -th level decoder.

Method	GlaS		MoNuSeg	
	Dice(%)	IoU(%)	Dice(%)	IoU(%)
U-Net (2015)	86.34	76.81	73.97	59.42
UNet++ (2018)	87.07	78.10	75.28	60.89
AttUNet (2018)	86.98	77.53	76.20	62.64
MRUNet (2020)	87.72	79.39	77.54	63.80
TransUNet (2021)	87.63	79.10	79.20	65.68
MedT (2021)	86.68	77.50	79.24	65.73
Swin-U-Net (2021)	88.25	79.86	78.49	64.72
<b>UCTransNet-pre</b>	<b>90.18</b>	<b>82.95</b>	77.19	63.80
<b>UCTransNet</b>	89.84	82.24	<b>79.87</b>	<b>66.68</b>

Table 1: Comparison with state-of-the-art segmentation methods on GlaS and MoNuSeg datasets. For simplicity, ‘AttUNet’ denotes Attention U-Net and ‘MRUNet’ denotes MultiResUNet. The best results are boldfaced.

Methods	Dice $\uparrow$	HD $\downarrow$
V-Net (2016)	68.81	-
DARR (2020)	69.77	-
U-Net (2015)	71.77	53.04
R50-U-Net	74.68	36.87
R50-AttUNet (2018)	75.57	36.97
TransUNet (2021)	77.48	31.69
UCTransNet (w/o CCA)	<b>78.99</b>	30.29
UCTransNet-pre	75.54	38.97
<b>UCTransNet</b>	78.23	<b>26.75</b>

Table 2: Comparison with state-of-the-art segmentation methods on Synapse dataset. For simplicity, ‘R50-U-Net’ and ‘R50-AttUNet’ denote U-Net and Attention U-Net with ResNet-50 as backbone, respectively.

## Experiments

### Datasets

We use Gland segmentation (Sirinukunwattana et al. 2016), MoNuSeg (Kumar et al. 2017, 2020) and Synapse multi-organ segmentation dataset (Bennett et al. 2015) to evaluate our method. Gland segmentation dataset (GlaS) has 85 images for training and 80 for testing. MoNuSeg dataset has 30 images for training and 14 for testing. Synapse has 30 abdominal CT scans in 8 abdominal organs (aorta, gallbladder, spleen, left kidney, right kidney, liver, pancreas, spleen, stomach), with 3779 axial CT images in total. Following (Chen et al. 2021), we use a random split of 18 training cases (2212 axial slices) and 12 cases for validation.

### Implementation Details

We implemented our model with PyTorch on a single NVIDIA A40 GPU card with 48 GB memory. To avoid overfitting, we also performed two kinds of online data augmentations, including horizontal flipping, vertical flipping and random rotating. We do not use any pre-trained weights to train the proposed UCTransNet. For GlaS and MoNuSeg we set the batch size to 4 following (Valanarasu et al. 2021), and

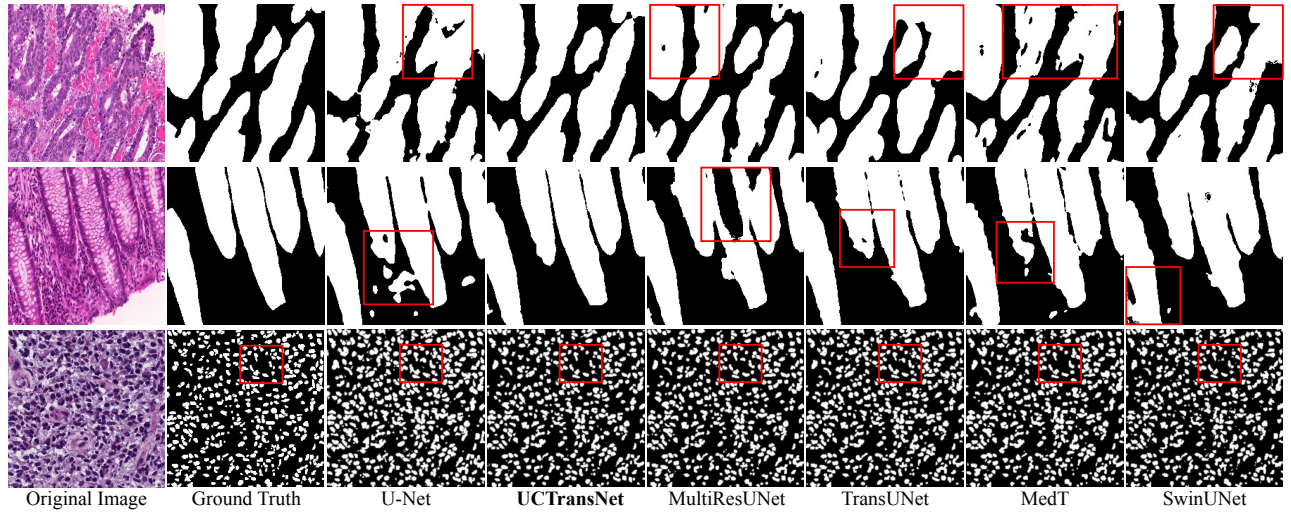


Figure 6: The qualitative comparison on the GlaS and MoNuSeg datasets.

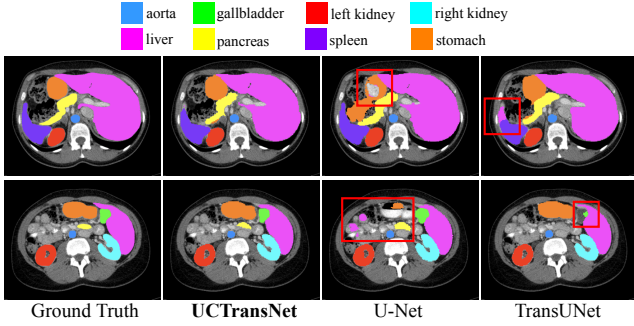


Figure 7: The qualitative comparison on the Synapse dataset.

for Synapse we set it to 24 following (Chen et al. 2021). The input resolution and patch size  $P$  are set as  $224 \times 224$  and 16 for all the three datasets. To obtain a fast convergence, we also employ the Adam optimizer to train our model, where the initial learning rate is set to 0.001. We employ the combined cross entropy loss and dice loss as our loss function to train our network. For GlaS and MoNuSeg datasets we use dice coefficient (Dice) and Intersection over Union (IoU) as the evaluation metrics while for Synapse we report the Dice and Hausdorff Distance (HD). Note that we use the same settings and loss function for training all the baselines.

### Comparison with State-of-the-art Methods

To demonstrate the overall segmentation performance of the proposed UTransNet, we compare it with other state-of-the-art methods. We compare UTransNet with two types of methods for comprehensive evaluation, covering three UNet based method: UNet++, Attention U-Net, MultiResUNet and three state-of-the-art transformer based segmentation methods, including TransUNet, MedT, and SwinUNet. To make a fair comparison, their originally released codes and published settings are used in the experiment. We also introduce two strategies to optimize the models of

UTransNet. 1) **Jointly training**: We optimize the convolution and CTrans parameters in U-Net and the two channel-wise cross attention parameters together with a single loss; 2) **Pre-training**. We first train a classical U-Net, then the overall parameters in UTransNet are further trained on the same data.

Experimental results are reported in Table 1 where the best results are boldfaced. Table 1 shows that our method has consistent improvements over prior arts, e.g. on GlaS dataset, performance gains range from 2.42% (3.59%) to 4.05% (7.07%) in terms of Dice (IoU) compared with the previous U-Net based models and from 1.80% (2.98%) to 3.65% (6.12%) in terms Dice (IoU) compared with the Transformer based models, respectively. In Table 2, similar observations and conclusions can be made, which once again validates that UTransNet outperforms all others. Additionally, the pre-training scheme not only achieves a faster convergence speed, but also obtains a better performance than the competing methods, even outperforms the jointly learning scheme on the MoNuSeg dataset. These observations suggest that the two proposed modules can be incorporated into the pre-trained U-Net model for improved segmentation performance.

We visualize the segmentation results of the comparable models in Fig. 6 and Fig. 7. The red boxes highlight regions where UTransNet performs better than the other methods. It shows that our UTransNet generates better segmentation results, which are more similar to the ground truth than the results of the baseline model. It can be easily seen that our proposed method not only highlights the right salient regions eliminating the confusing false positive lesions but also produces coherent boundaries. These observations suggest that UTransNet is capable of finer segmentation while preserving detailed shape information.

### Ablation Studies

To further investigate the relative contributions of each components, we conduct a series of experiments on both GlaS

Method	GlaS		MoNuSeg	
	Dice(%)	IoU(%)	Dice(%)	IoU(%)
Baseline (U-Net)	86.34	76.81	73.97	59.42
Baseline+CCT	89.09	80.78	79.31	65.97
Baseline+CCA	87.09	78.10	76.84	63.85
Baseline+CCT+CCA	<b>89.84</b>	<b>82.24</b>	<b>79.87</b>	<b>66.68</b>

Table 3: Ablation experiments on GlaS and MoNuSeg datasets. ‘CCT’ denotes the proposed Channel Transformer and ‘CCA’ denotes Channel-wise Cross Attention. The best results are boldfaced.

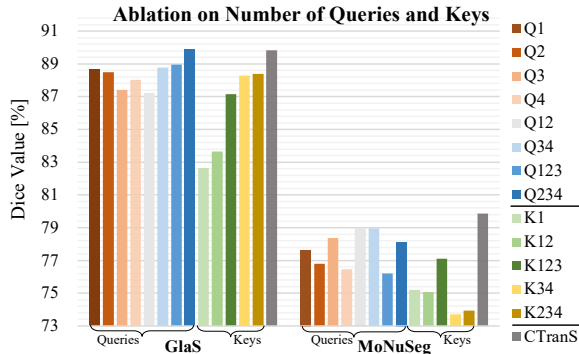


Figure 8: Ablation study of the number of queries and keys on GlaS dataset and MoNuSeg dataset.

and MoNuSeg datasets to investigate the individual contribution by removing each single module, varying the number of queries and key.

**Ablation Studies on Proposed Modules** As shown in Table 3, ‘Base+CCT+CCA’ is generally better than the other baselines on all datasets. By integrating CCT and CCA into U-Net, it improves 1.12% and 1.22% in Dice and IoU, respectively, which indicates the effectiveness of combination of the two modules. Our results shed new light on the importance of multi-scale multi-channel feature fusion in encoder-decoder framework for improving segmentation performance.

### Ablation Studies on the Number of Queries and Keys

The previous experiments demonstrate that the CCT module in our model is effective for enhancing the skip connections. In the previous experiments, the multi-scale features from all encoder levels engage into the CCT module, thus the number of queries is 4 and the key is the concatenated representation consisting of the four scale features.

We perform a series of experiments with respect to the amount of the skip connections between encoders and decoders as illustrated in Fig. 8. Note that the key vector is fixed, which is still consisting of the four scale features. We observe consistent improvements with the increase of the number of skip connections. The observation implies the usefulness of multi-scale features learned by different encoder levels, which validates our motivation. It is interesting that ‘Q234’ is slightly better than our model with

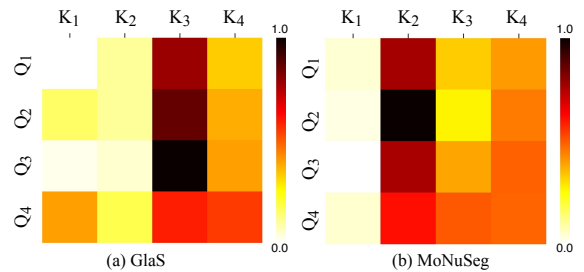


Figure 9: Similarity Matrix of GlaS dataset (a) and MoNuSeg dataset (b). ‘K<sub>1</sub>’ denotes the same feature as ‘Q<sub>1</sub>’ concatenated in key.

all skip connections. Besides, we also keep the number of queries fixed and vary the key to verify concatenating multi-scale features. From Fig. 8, it can be found that the performance improves with the scale of feature increasing until four scales, which demonstrates that more channels help capture accurate node features, which implies that transforming more scales of features to queries is better.

### The Cross Attention Matrix in CCT Module

To perform a thorough evaluation of our UCTransNet, we visualize the cross attention distributions in our CCT module in Fig. 9. It is also interesting to investigate which encoder level has more confident correlation and is more important for segmentation. It can be seen that the ‘K<sub>2</sub>’ and ‘K<sub>3</sub>’ have a more confident correlation with the other encoder level on the Glas and MoNuSeg dataset, respectively. The findings are consistent with the skip connection analysis in U-Net in Fig. 3. It explains why ‘L3’ and ‘L2’ achieve better performances on Glas and MoNuSeg dataset, respectively. The fact implies the necessity to develop a multi-scale feature fusion to tackle the semantic gap problems, which also validates our motivation to build a global multi-scale channel-wise feature fusion model for effectively capturing the non-local semantic dependencies.

## Conclusion

Accurate and automatic segmentation of medical images is a crucial step for clinical diagnosis and analysis. In this work, we introduced a Channel Transformer Segmentation network (UCTransNet) from the channel-wise perspective to provide precise and reliable automatic segmentation of medical images. By combining the strengths of multi-scale Channel-wise Cross fusion Transformer (CCT) and recurrent neural networks and Channel-wise Cross-Attention (CCA) in an end-to-end manner, the proposed approach significantly improves the state-of-the-art results in medical image segmentation on multiple benchmark datasets. With in-depth analysis and empirical evidence, we show the advantages of the UCTransNet model. It indeed successfully narrows the semantic gap and takes full advantage of the multi-scale features in the encoding stage.

## References

- Alom, M. Z.; Hasan, M.; Yakopcic, C.; Taha, T. M.; and Asari, V. K. 2018. Recurrent Residual Convolutional Neural Network Based on U-Net (R2U-Net) for Medical Image Segmentation. arXiv:1802.06955.
- Bennett, L.; Zhoubing, X.; Juan, I., Eugenio; Martin, S.; Thomas, L., Robin; and Arno, K. 2015. Segmentation Outside the Cranial Vault Challenge. In *MICCAI: Multi-Atlas Labeling Beyond Cranial Vault-Workshop Challenge (2015)*.
- Cao, H.; Wang, Y.; Chen, J.; Jiang, D.; Zhang, X.; Tian, Q.; and Wang, M. 2021. Swin-Unet: Unet-like Pure Transformer for Medical Image Segmentation. arXiv:2105.05537.
- Chen, J.; Lu, Y.; Yu, Q.; Luo, X.; Adeli, E.; Wang, Y.; Lu, L.; Yuille, A. L.; and Zhou, Y. 2021. TransUNet: Transformers Make Strong Encoders for Medical Image Segmentation. arXiv:2102.04306.
- Dosovitskiy, A.; Beyer, L.; Kolesnikov, A.; Weissenborn, D.; Zhai, X.; Unterthiner, T.; Dehghani, M.; Minderer, M.; Heigold, G.; Gelly, S.; Uszkoreit, J.; and Houlsby, N. 2020. An Image Is Worth 16x16 Words: Transformers for Image Recognition at Scale. arXiv:2010.11929.
- Drozdal, M.; Vorontsov, E.; Chartrand, G.; Kadoury, S.; and Pal, C. 2016. The Importance of Skip Connections in Biomedical Image Segmentation. In Carneiro, G.; Mateus, D.; Peter, L.; Bradley, A.; Tavares, J. M. R. S.; Belagiannis, V.; Papa, J. P.; Nascimento, J. C.; Loog, M.; Lu, Z.; Cardoso, J. S.; and Corneise, J., eds., *Deep Learning and Data Labeling for Medical Applications*, volume 10008, 179–187. Cham: Springer International Publishing. ISBN 978-3-319-46975-1 978-3-319-46976-8.
- Fu, S.; Lu, Y.; Wang, Y.; Zhou, Y.; Shen, W.; Fishman, E.; and Yuille, A. 2020. Domain adaptive relational reasoning for 3d multi-organ segmentation. In *Medical Image Computing and Computer Assisted Intervention – MICCAI 2020 - 23rd International Conference, Proceedings*, 656–666. Springer Science and Business Media Deutschland GmbH.
- Gao, Y.; Zhou, M.; and Metaxas, D. 2021. UTRNet: A Hybrid Transformer Architecture for Medical Image Segmentation. arXiv:2107.00781.
- Gao, Z.; Hong, B.; Zhang, X.; Li, Y.; Jia, C.; Wu, J.; Wang, C.; Meng, D.; and Li, C. 2021. Instance-Based Vision Transformer for Subtyping of Papillary Renal Cell Carcinoma in Histopathological Image. arXiv:2106.12265.
- Hatamizadeh, A.; Yang, D.; Roth, H.; and Xu, D. 2021. UNETR: Transformers for 3D Medical Image Segmentation. arXiv:2103.10504.
- He, K.; Zhang, X.; Ren, S.; and Sun, J. 2016. Deep Residual Learning for Image Recognition. In *2016 IEEE Conference on Computer Vision and Pattern Recognition (CVPR)*, 770–778. Las Vegas, NV, USA: IEEE. ISBN 978-1-4673-8851-1.
- Huang, G.; Liu, Z.; Van Der Maaten, L.; and Weinberger, K. Q. 2017. Densely Connected Convolutional Networks. In *2017 IEEE Conference on Computer Vision and Pattern Recognition (CVPR)*, 2261–2269. Honolulu, HI: IEEE. ISBN 978-1-5386-0457-1.
- Huang, H.; Lin, L.; Tong, R.; Hu, H.; Zhang, Q.; Iwamoto, Y.; Han, X.; Chen, Y.-W.; and Wu, J. 2020. UNet 3+: A Full-Scale Connected UNet for Medical Image Segmentation. arXiv:2004.08790.
- Ji, Y.; Zhang, R.; Wang, H.; Li, Z.; Wu, L.; Zhang, S.; and Luo, P. 2021. Multi-Compound Transformer for Accurate Biomedical Image Segmentation. arXiv:2106.14385.
- Kumar, N.; Verma, R.; Anand, D.; Zhou, Y.; Onder, O. F.; Tsougenis, E.; Chen, H.; Heng, P.-A.; Li, J.; and Hu, Z. 2020. A Multi-Organ Nucleus Segmentation Challenge. *IEEE Transactions on Medical Imaging*, 39(5): 1380–1391.
- Kumar, N.; Verma, R.; Sharma, S.; Bhargava, S.; Vahadane, A.; and Sethi, A. 2017. A Dataset and a Technique for Generalized Nuclear Segmentation for Computational Pathology. *IEEE Transactions on Medical Imaging*, 36(7): 1550–1560.
- Li, X.; Chen, H.; Qi, X.; Dou, Q.; Fu, C.-W.; and Heng, P.-A. 2018. H-DenseUNet: Hybrid Densely Connected UNet for Liver and Tumor Segmentation From CT Volumes. *IEEE Transactions on Medical Imaging*, 37(12): 2663–2674.
- Liu, Z.; Lin, Y.; Cao, Y.; Hu, H.; Wei, Y.; Zhang, Z.; Lin, S.; and Guo, B. 2021. Swin Transformer: Hierarchical Vision Transformer using Shifted Windows. arXiv:2103.14030.
- Long, J.; Shelhamer, E.; and Darrell, T. 2015. Fully Convolutional Networks for Semantic Segmentation. *CVPR*, 10.
- Milletari, F.; Navab, N.; and Ahmadi, S.-A. 2016. V-Net: Fully Convolutional Neural Networks for Volumetric Medical Image Segmentation. arXiv:1606.04797.
- Ni, Z.-L.; Bian, G.-B.; Wang, G.-A.; Zhou, X.-H.; Hou, Z.-G.; Chen, H.-B.; and Xie, X.-L. 2020. Pyramid Attention Aggregation Network for Semantic Segmentation of Surgical Instruments. *Proceedings of the AAAI Conference on Artificial Intelligence*, 34(07): 11782–11790.
- Oktay, O.; Schlemper, J.; Folgoc, L. L.; Lee, M.; Heinrich, M.; Misawa, K.; Mori, K.; McDonagh, S.; Hammerla, N. Y.; Kainz, B.; Glocker, B.; and Rueckert, D. 2018. Attention U-Net: Learning Where to Look for the Pancreas. arXiv:1804.03999.
- Rahman, M. S. 2020. MultiResUNet : Rethinking the U-Net Architecture for Multimodal Biomedical Image Segmentation. *Neural Networks*, 121: 74–87.
- Ronneberger, O.; Fischer, P.; and Brox, T. 2015. U-Net: Convolutional Networks for Biomedical Image Segmentation. arXiv:1505.04597.
- Sirinukunwattana, K.; Pluim, J. P. W.; Chen, H.; Qi, X.; Heng, P.-A.; Guo, Y. B.; Wang, L. Y.; Matuszewski, B. J.; Bruni, E.; Sanchez, U.; Böhm, A.; Ronneberger, O.; Cheikh, B. B.; Racoceanu, D.; Kainz, P.; Pfeiffer, M.; Urschler, M.; Snead, D. R. J.; and Rajpoot, N. M. 2016. Gland Segmentation in Colon Histology Images: The GlAS Challenge Contest. arXiv:1603.00275.
- Ulyanov, D.; Vedaldi, A.; and Lempitsky, V. 2017. Instance Normalization: The Missing Ingredient for Fast Stylization. arXiv:1607.08022.
- Valanarasu, J. M. J.; Oza, P.; Hacihaliloglu, I.; and Patel, V. M. 2021. Medical Transformer: Gated Axial-Attention for Medical Image Segmentation. arXiv:2102.10662.



Wang, Q.; Wu, B.; Zhu, P.; Li, P.; Zuo, W.; and Hu, Q. 2020. ECA-Net: Efficient Channel Attention for Deep Convolutional Neural Networks. In *2020 IEEE/CVF Conference on Computer Vision and Pattern Recognition (CVPR)*, 11531–11539. Seattle, WA, USA: IEEE. ISBN 978-1-72817-168-5.

Wen, Y.; Xie, K.; and He, L. 2020. Segmenting Medical MRI via Recurrent Decoding Cell. *Proceedings of the AAAI Conference on Artificial Intelligence*, 34(07): 12452–12459.

Zhang, Y.; Higashita, R.; Fu, H.; Xu, Y.; Zhang, Y.; Liu, H.; Zhang, J.; and Liu, J. 2021. A Multi-Branch Hybrid Transformer Network for Corneal Endothelial Cell Segmentation. arXiv:2106.07557.

Zhang, Y.; Liu, H.; and Hu, Q. 2021. TransFuse: Fusing Transformers and CNNs for Medical Image Segmentation. arXiv:2102.08005.

Zheng, S.; Lu, J.; Zhao, H.; Zhu, X.; Luo, Z.; Wang, Y.; Fu, Y.; Feng, J.; Xiang, T.; Torr, P. H. S.; and Zhang, L. 2020. Rethinking Semantic Segmentation from a Sequence-to-Sequence Perspective with Transformers. arXiv:2012.15840.

Zhou, Z.; Siddiquee, M. R.; Tajbakhsh, N.; and Liang, J. 2018. UNet++: A Nested U-Net Architecture for Medical Image Segmentation. *DLMI/ML-CDS@MICCAI*.